


Cooperative Behavior in the Evolution of Alignment and Structure in Vertically Aligned Carbon-Nanotube Arrays Grown using Chemical Vapor Deposition

Gyula Eres,^{1,2,*} C.M. Rouleau,² A.A. Puretzky,² D.B. Geohegan,² and H. Wang³

¹*Materials Science and Technology Division, Oak Ridge National Laboratory, Oak Ridge, Tennessee 37831, USA*

²*Center for Nanophase Materials Sciences, Oak Ridge National Laboratory, Oak Ridge, Tennessee 37831, USA*

³*Department of Mechanical Engineering, Binghamton University, State University of New York, Binghamton, New York 13902, USA*

 (Received 24 August 2017; revised manuscript received 29 January 2018; published 10 August 2018)

This paper is a contribution to the [Physical Review Applied collection](#) in memory of Mildred S. Dresselhaus.

We discuss the origin and the influence of autocatalytic kinetics on the structure-property relationship in the evolution of macromolecular structure during self-organized growth of vertically aligned carbon-nanotube arrays by chemical vapor deposition of acetylene. Real-time thickness measurements consistent with postgrowth structural characterization show that the rate of carbon incorporation governs not just the length of individual nanotubes, but also cooperative properties such as packing density, alignment, and order in the arrays, which profoundly affect the mechanical strength and the thermal and electrical conductivity of the assembly. Our analysis shows that the autocatalytic kinetics points to radical chain polymerization of acetylene as the most likely mechanism capable of producing the large variations in carbon-addition rates revealed by real-time data. This fresh insight provides alternative approaches for targeting specific array properties using the polymerization reaction framework for creating novel applications in high-density energy storage, advanced interconnects, and high-efficiency heat dissipation.

DOI: [10.1103/PhysRevApplied.10.024010](https://doi.org/10.1103/PhysRevApplied.10.024010)

I. INTRODUCTION

The growth of dense highly ordered vertically aligned nanotube arrays (VANTA) or nanotube forests by chemical vapor deposition (CVD) represents one of the most significant achievements in carbon-nanotube (CNT) synthesis [1,2]. This growth mode is attractive because it provides great versatility for controlling the synthesis process, and represents a highly flexible platform for developing applications [2]. The catalytic surface region remains physically separated from the growing CNTs, simplifying or totally eliminating the need for postgrowth purification and catalyst-particle removal. The growth of individual CNTs occurs by self-assembly of carbon species that governs the macromolecular structure on different length scales creating self-organized assemblies of fascinating complexity reflected in macroscopic properties such as packing density, alignment, and order [3]. Here we explore the role of CNT growth kinetics on the properties and functionality of the VANTA and discuss how it can be harnessed for developing advanced technologies based on exploiting the extraordinary properties of individual carbon nanotubes in collective assemblies [2,4].

The most challenging problems in CNT research are related to the fundamental understanding of the CNT

growth mechanisms that still remain unsolved three decades after their discovery [5]. Specifically, these challenges include controlling chirality, diameter, number of walls, and length by the synthesis process [2,5]. While the nucleation step is specific to the nature and the morphology of the catalyst particles, including interactions with the catalyst support, carbon incorporation is a reaction step commonly shared by all CNT growth processes. Here we show that bypassing the difficult problem of nucleation and addressing only the growth stage that is driven by the addition of carbon to the CNT walls (incorporation reaction) provides important insight for overcoming the termination problem that plagues forest growth.

Although we are not directly creating applications in this work, we are laying down the foundation for applications by identifying key factors that affect properties and functionality of VANTA during growth. In the growth of forests in general, the kinetics of carbon incorporation and the dynamics of structure formation are intertwined. The sigmoidal shape of the growth curves has a special significance for both of these processes [6]. In this paper we first discuss possible origins of sigmoidal behavior for each process separately. However, we stress that in actual growth the overlap and the interdependence of carbon kinetics and the formation of structure are critical for understanding and controlling the evolution of the properties and functionality of the VANTA. It is clear that

*eresg@ornl.gov

in real growth the two are not separable. Unraveling the interplay between carbon kinetics and formation of structure requires experiments capable of characterizing forest growth in real time that are currently being developed and implemented to measure simultaneously catalyst composition, particle size, and CNT diameter distribution and the forests' structural evolution dynamics [7,8].

It is a particularly intriguing question whether there is a growth regime in which a dominant mechanism is responsible for the sigmoidal behavior. The formation of structure is important because the forests are not just an assembly of noninteracting “sticks.” A good entry point for starting the discussion about the structure and the interactions of CNTs in the growing arrays is the analogy with the “bed of nails” configuration. Allowing a nonperiodic distribution of spacings and different growth rates of individual elements or “nails” in addition to bending, overlapping, and twisting illustrates well the picture of individual CNT growth. However, in addition to growth of individual units there is also bundle formation and bending that involve collective behavior, which also lead to sigmoidal growth behavior. Based on the autocatalytic kinetics we propose radical chain polymerization of acetylene as the most likely reaction for carbon incorporation in individual CNT growth. The polymerization reaction spontaneously results in a distribution of products in a form of individual CNTs with different growth rates, diameters, and lengths [9], which intrinsically creates the conditions for cooperative behavior in structure formation and evolution that is indicated by the sigmoidal growth curves that ultimately describe properties and functionality.

II. EXPERIMENTAL METHODS

The data in Fig. 1 illustrate real-time imaging of VANTA growth using time-lapse videography performed

by a CCD camera set to continuously capture edge-on images at a desired frame rate. VANTA growth on metal catalyst films consisting of 10 nm Al and 1 nm Fe deposited on a Si wafer is performed by acetylene (C_2H_2) CVD assisted by trace amounts of ferrocene $[(C_5H_5)_2Fe]$ [10]. A series of frames depicted in Fig. 1(a) illustrates construction of time-dependent growth curves for studying the kinetics of VANTA growth. The sequential frames in Fig. 1(a) reveal highly selective VANTA growth that even after 5 h occurs only on the area defined by the metal catalyst film. Practical experience shows that growth selectivity is a critical prerequisite for high-quality VANTA growth. The high degree of selectivity indicates the dominance of the heterogeneous component of acetylene pyrolysis under these conditions. Any accumulation of carbon on the inactive Si surface is a sign of undesirable departure from ideal VANTA growth conditions and occurs when gas-phase pyrolysis (homogeneous component) takes over and produces soot. The typical growth data illustrated in Fig. 1(b) describe the VANTA height as a function of time, representative of the time-dependent carbon uptake by the growing CNTs. The defining feature of these data is the highly nonlinear nature of the S-shaped sigmoidal growth curves. These growth curves are similar to those obtained by other real-time measurement techniques of the height evolution including laser optical reflectivity [3] and grazing-incidence small-angle x-ray scattering (GISAXS) [11].

The sigmoidal curves represent a mathematical description of cooperative behavior that occurs during formation of complex self-assembled structures [6]. Cooperative behavior in growth processes is widespread in nature and it is ubiquitous in systems that involve C—C bonding. The resulting S-shaped growth curves of CNT forests are fitted using several different functions including logistic, Gompertz [12], and others. Although the changes of the purely

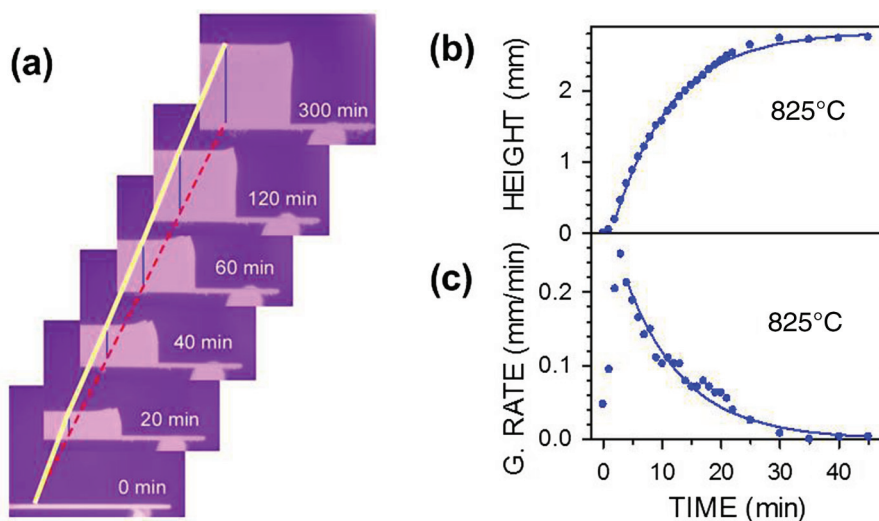


FIG. 1. (a) A sequence of edge-on CCD camera images of VANTA growth in real time. A 0.4-mm-thick Si wafer is shown resting on a ceramic boat at time zero. The VANTA height after 300 min is 7.5 mm. The thick yellow line illustrates the VANTA height envelope as a function of time. (b) Example sigmoidal shape curve for VANTA growth at 825°C. (c) The growth-rate change with time obtained by numerical differentiation of the growth curve in (b), showing first a brief ~ 5 -min acceleration stage, followed by a protracted decay of the growth rate.

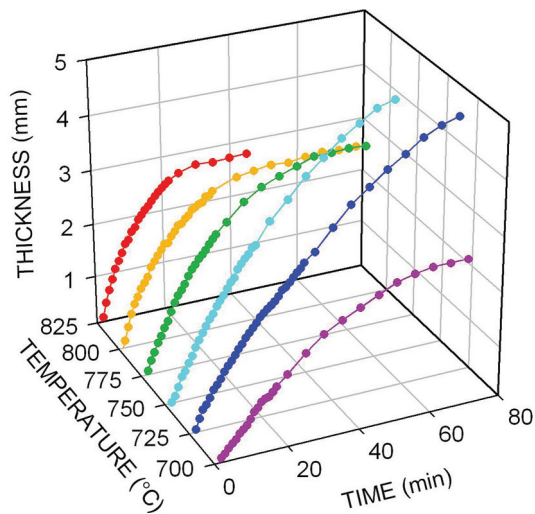


FIG. 2. 3D plot of the temperature dependence of the growth curves in the range from 700 to 825 °C. The solid lines are guides to the eye. The VANTA growth is performed in a flow of 500 sccm of He, 100 sccm of H₂, 12.4 sccm of C₂H₂, and a $\sim 10^3$ ratio of C₂H₂/[(C₅H₅)₂Fe] at atmospheric pressure.

mathematical fitting parameters can be measured experimentally, they provide no meaningful insight because of a lack of connection to a physical model [6]. The physical models are crucial because cooperative behavior in molecular self-assembly typically arises from the coupling of two or more inherently simple steps, which can be isolated by standard physical methods and analyzed quantitatively [13]. An additional requirement for making the model meaningful is to restrict to a minimum the number of parameters needed for achieving a good fit.

The kinetics described by the sigmoidal shape of the growth curves persists for a wide range of growth conditions including incidence rate, temperature, and type of carbon source molecule. The 3D plots of the data in Fig. 2 illustrate dramatic changes in the shape of the growth curves as the temperature increases from 700 to 825 °C. However, the growth curves preserve the common features that are representative of the underlying kinetics. The sigmoidal growth curves represent processes that have three stages including an induction-delay, a growth-acceleration stage, and a slow-growth termination stage [6]. The transition from one stage into the next occurs as the reaction proceeds and is marked by inflection points that are revealed in Fig. 1(b) by numerical differentiation of the growth curves. The significance of real-time monitoring is that it captures brief but important time-dependent features (transients) that could go unnoticed in studies using arrested-growth techniques. However, the resulting growth-rate curve in Fig. 1(c) shows only two segments corresponding to the growth-acceleration and the growth-termination stages. The induction delay, which is a slow reaction stage

that occurs at the onset of the growth, is often missing in real-time data because the experimental resolution is inadequate to capture the slow growth of very short VANTA. The induction-delay stage continues into the growth-acceleration stage that is widely recognized in carbon deposition. The CVD method in which growth acceleration is attributed to water-molecule-assisted “cleansing” of the catalyst particle surface to regenerate lost catalytic activity is called “supergrowth” [14]. However, with the availability of real-time data from other growth experiments that do not use water, such as these, it becomes clear that although supergrowth is important, it is just a brief accelerating stage in the overall kinetics of VANTA growth.

III. RESULTS AND DISCUSSION

The two separate growth segments in Fig. 1(c) clearly illustrate why the standard model that balances the activation and the deactivation steps is so appealing and widely used. This model is one that was originally developed for the interpretation of catalytic carbon deposition on Ni-coated carbon filaments that shows growth behavior similar to VANTA [15]. The series of rate equations set up in the model also postulates, in addition to active and inactive sites, the existence of sites that are responsible for poisoning the catalyst surface and causing growth termination. The reaction sequence is completed by including adsorption and desorption of hydrocarbon and hydrogen, hydrogenation and dehydrogenation surface reactions, and carbon dissolution, diffusion, and precipitation. Although these models can produce quite satisfactory fitting of experimental data, they fail to provide mechanistic insight because of the overwhelming number of *ad hoc* steps and fitting parameters. However, the main weakness of these types of models is that they neglect molecular processes and address only the growth of isolated (individual) CNTs [16]. A widely used model that also treats only the growth of individual CNTs is based on the dissolution-precipitation process that is transplanted from the days of carbon-filament growth [17]. The relevance of this model for CNT growth is not firmly established. The essential feature of this mechanism is that CNT growth occurs by precipitation of atomic carbon that is first dissolved by a metal catalyst particle. While this can certainly occur with those metals that dissolve carbon, recent numerous reports of CNT growth from materials including semiconductors and ceramics that do not dissolve carbon rule out dissolution or precipitation as a general mechanism for CNT growth [18]. Moreover, a demonstration of CNT formation from molecular fragments on a flat surface implies that catalyst particles are not indispensable [18,19]. Currently very few models address the effects of growth kinetics on the collective

properties of VANTA forming by spontaneous vertical alignment [20].

A. Observation of Autocatalytic Kinetics in VANTA Growth

Ideally, the goal for any study of reaction kinetics is to determine the sequence of chemical bonding changes that transform the molecular structure of reactants into products. Practical experience shows that CVD of CNTs, similar to other carbon pyrolysis processes, involves numerous intermediates produced by complex reaction sequences that makes isolation of a rate-limiting step daunting. Guided by the adage that kinetics can never prove a mechanism just eliminate alternative pathways, we follow the principle of Occam's razor in considering the remaining reaction types consistent with the real-time data [21]. By identifying the reaction type, it is still possible to learn a lot about the reaction, because in general, a particular reaction type is associated with specific products. The significance of the sigmoidal growth curves is that carbon addition occurs at continuously changing rates. A type of reaction that naturally exhibits all three stages observed in VANTA growth without needing *ad hoc* assumptions is autocatalysis. Autocatalytic reactions are unique in that their product is also the reactant, that is, the reaction is catalyzed by its own products [22]. In contrast to first- and second-order reactions in which the reaction is fastest at the start, autocatalytic reactions are slow at the onset because very little product is present.

In VANTA growth, the autocatalytic kinetics is tied to the unique role that C_2H_2 plays in carbon nanostructure formation. Using a molecular beam to determine the reaction probability on a single-collision level, we were able to show that C_2H_2 is the most efficient carbon source molecule for VANTA growth [23]. This finding was confirmed independently by many other experiments, showing that for efficient VANTA growth, C_2H_2 must form as a key intermediate if the source molecule is a hydrocarbon other than C_2H_2 [24]. In the reaction



where P_n is the CNT product, and $n \gg 1$ signifies that the reaction produces a distribution of CNTs with different properties. The rate law

$$v = k[A][P_n] \quad (2)$$

shows that the reaction rate increases with the formation of products. The reaction is started because there are other reaction pathways that initially form some P_n that participate in the autocatalytic reaction. In the case of CNT growth such reactions involve nucleation of the CNT cap with an already started wall segment [3]. After a molecule

of C_2H_2 is added to extend the wall of such a CNT and desorption of H_2 is completed, the resulting product becomes a replica of the starting CNT, and it again becomes a reactant in the autocatalytic step. The solution of the differential equation for the rate law after substituting for $[A] = [A]_0 - x$, and $[P_n] = [P_n]_0 + x$ is given by

$$\frac{x}{[P_n]_0} = \frac{e^{at} - 1}{1 + e^{bt}}, \quad (3)$$

where x is the rate of product formation, $[A]_0$ is the concentration of reactant $[A]$, and $[P_n]_0$ is the concentration of product $[P_n]$ at $t = 0$, giving the parameters $a = ([A]_0 + [P_n]_0)k$, and $b = [P_n]_0/[A]_0$ [25]. The reaction rate is affected not just by the rate constant k (set by the temperature) but also by the initial concentration of the products $[P_n]_0$. The reaction starts slowly because $[P_n]_0$ is small. It accelerates as the concentration of the product that is also a reactant increases and slows down as the reactant is exhausted. Note that in real growth, parameters a and b are temperature dependent and, along with k , determine the shape of the growth curves. The concentration dependence of a and b accounts for the sensitivity of the experimental induction delay on the C_2H_2 pressure. Comparison of the curves in Fig. 3 with the experimental data in Fig. 2 shows that the two parameters a and b completely capture all the trends in the evolution of experimental growth curves. A particularly interesting and unexpected experimental trend is the decreasing array height with increasing temperature, accompanied by a single-exponential-like appearance of the growth curves. This behavior is found to be widespread in many growth methods and is formulated into a rule of inverse relationship between the CNT growth rate and the catalyst lifetime [26]. An increasing parameter a (at fixed b) captures the exponential shape, and increasing b (at fixed a) takes care of interpreting the decreasing total product amount as well as removing the induction delay responsible for the sigmoidal shape.

B. Autocatalytic Behavior of Acetylene Polymerization in VANTA Growth

The purpose of exploring the kinetics is to eliminate as many pathways as possible and narrow down the possibilities to a few, preferably only a single, plausible molecular mechanism. Autocatalytic behavior in carbon deposition involving C_2H_2 is already reported in work from 1970 [27]. The overall yield curves of carbon-fiber growth on metal wires show similar trends as VANTA growth as a function of temperature, clearly exhibiting an acceleration stage followed by a slowdown of growth. Autocatalytic behavior and similar highly nonlinear yield curves are observed also in soot growth from C_2H_2 and other small hydrocarbon molecules [28]. If autocatalytic behavior occurs both in the presence and absence of metal

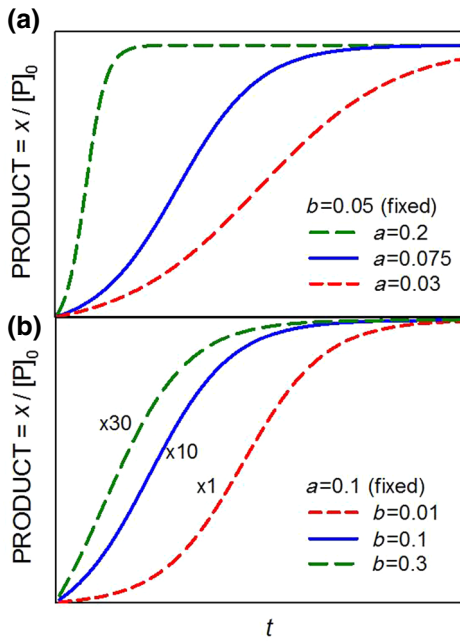


FIG. 3. The change of the shape of the sigmoidal growth curves as a function of the parameters a and b of the autocatalytic reaction model. (a) Note that increasing a at fixed b amounts to increasing k by increasing the temperature. However, the sigmoidal shape caused by the induction period remains. (b) The sigmoidal shape is removed by increasing b at fixed a . But this also results in a proportional decrease in the final product amount (saturation value of x), by a factor given next to each particular curve.

particles, it cannot be attributed solely to catalyst activation and instead it must be related to reactions intrinsic to C_2H_2 . There is overwhelming experimental data on C_2H_2 thermal decomposition showing that the autocatalytic behavior is related to some type of “polymerization” process. There are extensive studies of molecular level mechanisms of thermally induced C_2H_2 polymerization, but the process is so complex that the role of various steps remains unresolved and controversial [29]. Regardless of the exact molecular mechanism, the C_2H_2 polymerization reaction in initiation, propagation, and termination exhibits the same three reaction stages that are also observed in VANTA growth kinetics. Consistent with the experimentally observed kinetics features of VANTA growth, polymerization is a reaction capable of sequentially adding carbon at a self-accelerating rate. In addition to similarities in reaction kinetics and mechanistic details, there are also great similarities in morphological features between polymerization products and CNT growth. There is an uncanny resemblance in the morphology of polyacetylene fibrils and vertically aligned carbon-nanotube arrays. The cracks in polyacetylene films reveal aligned or partially aligned fibers of 5–40-nm-diameter bridging the gaps, much like in CNT forests [30].

The key product that polymerization reactions of C_2H_2 produce is aromatic carbon. Aromatic carbon species are the well-known precursors of fullerenes and related sp^2 networks. The implications of the kinetics is that carbon incorporation into CNT walls and aromatic carbon formation share similar reaction mechanisms and reaction steps. There are extensive studies on the formation of aromatic carbon in connection with soot-formation mechanisms and soot kinetics as mentioned earlier. The main mechanism in soot formation is found to be the addition of C_2H_2 in concert with removal of a H atom, a mechanism referred to as hydrogen abstraction acetylene addition or HACA for short [31]. Over time, this mechanism gained widespread acceptance as a hypothesis for aromatic carbon formation. However, the exact mechanism still lacks direct experimental proof. Up to now, only formation of the second ring is proven by direct observation of acetylene addition to one-ringed phenyl radicals [32].

It is now generally accepted that the dominant mechanism for carbon addition in CNT CVD also involves C_2 species [23,24,33]. Unlike the random structure of soot, the molecular structure of CNTs is highly ordered, making the exact location of the C_2 species addition to the carbon network very important. In theoretical modeling of CNT growth, we find that removing hydrogen from acetylene intermediates to create active sites for such addition is very difficult [33]. However, the addition of C_2 species alone even after cap formation is found to be favorable [34]. It is also found that structural disorder existing at a growing CNT rim during growth plays a role of intermediate configurations that facilitate addition of reactive carbon species that are necessary for reaction propagation [35].

C. The Role of Polymerization in Governing the VANTA Properties

There is an intriguing relationship between the polymerization parameters and VANTA height and structure that is connected to the sigmoidal shape of the growth curves and the time constants exhibited by VANTA growth in Fig. 4. The increase in VANTA height by a polymerization reaction is proportional to the number of C_2H_2 molecules that are incorporated per active carbon radical site. This number is given by the kinetic chain length (ν) for polymerization $\nu = R_p/R_t$, where R_p is the propagation rate and R_t the termination rate [9]. The termination process is a pseudo-first-order reaction, with a lifetime given by τ_t , illustrated in Fig. 4(b). In the catalyst-particle-centric growth models τ_t is treated as the catalyst lifetime [26]. Assuming that the propagation step is represented by a time constant τ_p , the kinetic chain length is given by $\nu = \tau_t/\tau_p$ [9,22]. The propagation rate is proportional to the rate of disappearance of monomer (C_2H_2), which is difficult to measure in VANTA growth experiments. However, it is important to note that ν increases during the

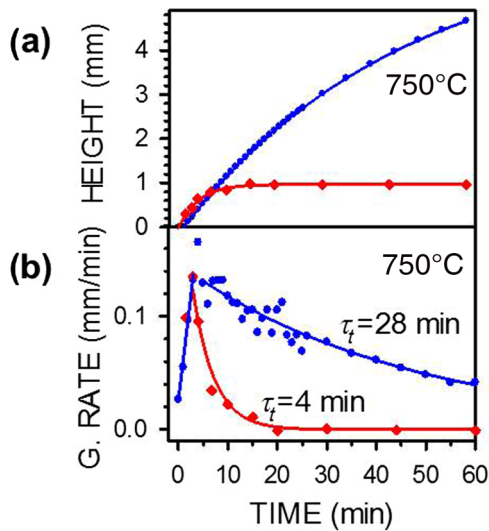


FIG. 4. Comparison of the time constants in water-assisted growth (red lines and symbols) and ferrocene-assisted growth (blue lines and symbols) at 750°C. (a) Growth curves as a function of time. Note that the height of ferrocene-assisted growth after termination is ~ 7.5 mm. (b) Growth-rate curves as a function of time, where τ_t corresponds to the termination time constant.

acceleration stage and tails off during the termination stage of the reaction. Since the duration of most VANTA growth is such that the overall kinetics is dominated by the termination step, $\nu \approx \tau_t$ represents a good approximation for the kinetic chain length, and it is a good predictor of the final VANTA height. The ratio of the τ_t for ferrocene-assisted and water-assisted growth in Fig. 4(b) of $28/4 = 7$ roughly matches the height ratio of the two arrays of 7.5. However, ν has a broader significance than just describing the VANTA height [9]. Analogous to conventional polymerization, the kinetic chain length describes the extent of polymerization, which governs the mechanical strength and other physical properties. Specifically for VANTA the extent of polymerization is a predictor of the length and the type of CNTs in the VANTA including their cooperative behavior that affects alignment and anisotropy that govern physical properties of interest for applications such as mechanical strength, thermal, and electrical conductivity.

A feature highly relevant for developing technological applications by direct VANTA growth is the distribution of individual CNT properties such as length, diameter, and wall number produced by a polymerization reaction. A unique function of the VANTA growth configuration is to “compress” these distributions during growth within the physical boundaries created by the VANTA thickness. The most obvious example of such compression is the bending of individual CNTs and the undulation of bundles that grow faster than the average VANTA growth rate. Collectively this behavior adversely affects alignment and anisotropy in the VANTA first studied by postgrowth

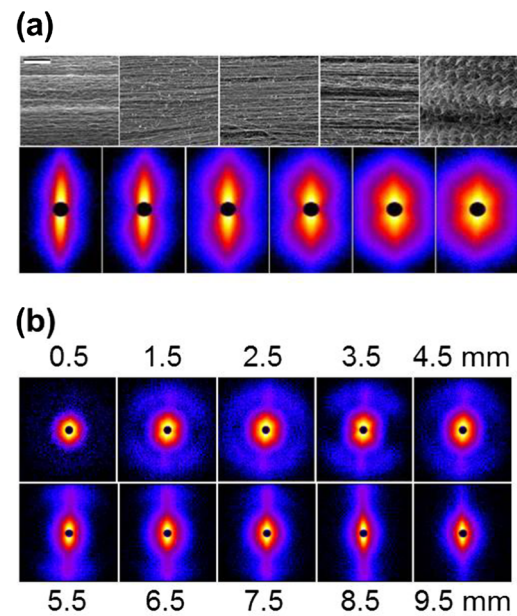


FIG. 5. Characterization of order in VANTA by SANS measurements. (a) From left to right, the top row shows SEM images from the top to the bottom of the VANTA. The scale bar for the SEM images is $2 \mu\text{m}$. The increasing disorder is manifested in the neutron scattering intensity profiles (second row) that change (left to right) from an elongated shape for straight CNTs to a more round isotropic distribution with CNTs becoming wiggly. For details of the measurements and data analysis see Ref. [36]. (b) SANS measurements of a 10 mm array after self-termination of growth. Zero is at the substrate at the root of the VANTA.

analysis and subsequently characterized *in situ* by real-time measurements [7,36]. Our postgrowth small angle neutron scattering (SANS) data show in Fig. 5(a) that loss of alignment and disorder increases with growth time as VANTA height increases [36]. Since carbon incorporation occurs at the root, the quality of individual CNTs in VANTA gradually deteriorates from the top to the bottom. In the extreme case of arrays that self-terminate illustrated in Fig. 5(b), the carbon distribution near the root area of a 10-mm-tall VANTA becomes completely isotropic. In essence, CNT growth degenerates into random carbon-nanostructure growth.

The buildup of disorder at the bottom is a well-known feature of VANTA growth that also must be related to the mechanism and the rate of carbon addition that cannot be addressed by the isolated CNT growth models, which are restricted to carbon incorporation only into the CNT walls. Disorder formation is an integral part of the polymerization process, and it builds up as the reaction proceeds. The rate of sequential addition of C_2 reactive species is crucial for understanding disorder formation on a molecular level. If the reaction accelerates too fast, it is likely to produce short VANTA and highly disordered growth [35]. The autocatalytic model describes this scenario by an increasing

b at fixed a as illustrated in Fig. 3(b). This is a characteristic feature of radical chain polymerization, which once initiated propagates by addition of more and more C_2H_2 molecules at active sites generated by the addition of C_2H_2 molecules. If this feedback process becomes too intense, it can run out of control and lead to an explosion, which is a well-known safety problem in C_2H_2 handling and storage. On the other hand, this feature of the C_2H_2 chain reaction is exploited for the synthesis of catalyst-free high-quality graphene flakes in a method referred to as gas-phase hydrocarbon detonation [37]. In typical VANTA growth the acceleration step is designed to fizzle out to prevent the chain reaction from running out of control. But a drawback in this regime is that the reaction runs out of active sites where C_2H_2 addition can occur. Multiple reaction pathways can operate concurrently wherein chains grow at different rates and crosslink or branch before they can be incorporated into the CNT walls, resulting in a growth process manifested by increasing disorder in the growing structures. The slowdown in carbon incorporation into CNT side walls, because of active site depletion, causes the accumulation of unprocessed carbon in the bottom region of VANTA. The result of this type of disordered growth is degradation of anisotropic thermal and electrical conductivity of both individual CNTs and VANTAs.

The above discussion shows that CNT growth shares important characteristics with soot growth, another sp^2 carbon structure that only differs in size and degree of order of the sp^2 network and grows by the same mechanism that produces aromatics. Similar to CNTs, deceleration and termination also occur in soot growth, which is referred to as “surface aging” [31]. The autocatalytic kinetics is consistent with these mechanistic features and shows that the growth of aromatics has the intrinsic ability to exhaust the supply of reactive sites needed for propagating its own growth. Recent data obtained by monitoring the growth of a single CNT by *in situ* TEM imaging reveal that growth termination is intrinsic to CNT growth from hydrocarbons [38]. Within the framework of radical chain polymerization, growth termination occurs because all the active sites for carbon addition are depleted by complete hydrogen desorption.

Although the main features of the carbon-addition kinetics are similar, an important distinction is that soot growth occurs by homogeneous polymerization and VANTA growth by heterogeneous polymerization. The growth selectivity imposed by the film implies that the surface of the film plays a critical role in the initiation of the process and the subsequent propagation of the chemical pathways that favor VANTA growth. The kinetic data suggest that the dissolution-precipitation model is a gross oversimplification that is inadequate for describing the complex processes of nucleation and carbon addition in VANTA growth. The catalyst in heterogeneous polymerization plays a dual role that includes regulating the rate

and the mechanism of carbon addition on the molecular level. The induction period at the onset during which the rate accelerates is an important feature of this reaction [39]. During the induction period, the concentration of free radicals builds up to a steady state. The exact chemical species and the mechanism by which acetylene pyrolysis is initiated remain a controversial topic even after several decades of active research [29,39,40]. However, important clues are revealed by the factors that affect the reaction rate during the induction period.

D. Novel Mechanisms for Extended VANTA Growth by Preventing Growth Termination

The peak growth rate at the end of the acceleration period increases with temperature. The low activation energy of (0.3 ± 0.1) eV of this step is indicative of free radical polymerization [39]. Similar activation energies are obtained in free radical polymerization of ethylene and propylene in the gas phase. Another common feature that VANTA growth shares with olefin and acetylene polymerization reactions is the prominent role that initiators play in starting the reaction [41]. Oxygen-containing species are well-known initiators of polymerization. However, the reaction of oxygen species with unsaturated hydrocarbons is a complex and delicate process. Influenced by a wide range of factors, the type and the level of oxygen species can have unpredictable consequences and even switch from initiators to inhibitors. We find that *in situ* oxidation of the metal catalyst films by exposure of the reactor interior to ambient air during the heating stage is critical for obtaining the tallest VANTA [42]. In addition, a deliberate supply of water vapor above atmospheric humidity during the heating stage is occasionally found to amplify the effect of ambient catalyst oxidation. This observation is in agreement with the supergrowth experiments where addition of more water above the initial enhancement level have no further effect on the growth rates [41]. In Fig. 4 the data for water-assisted growth are replotted and compared with VANTA growth rates. The fact that VANTA growth and supergrowth kinetics exhibit such great similarity during the acceleration stage suggests that polymerization is the key to the unexpected growth enhancement in the early stages of water-assisted growth. This similarity raises the interesting question of whether water-assisted growth occurs by direct polymerization of ethylene, or ethylene must be first converted to acetylene before polymerization occurs. Indeed, it is reported that thermal cracking of ethylene-containing feedstock in a temperature range from 860 to 1240 °C, and cooling it down to lower temperatures before introducing it onto a heated metal catalyst film results in substantially increased CNT growth rates [43]. The growth-rate increase measured in real time is correlated with an abundance of acetylenic species such as methyl acetylene and vinyl acetylene that are detected

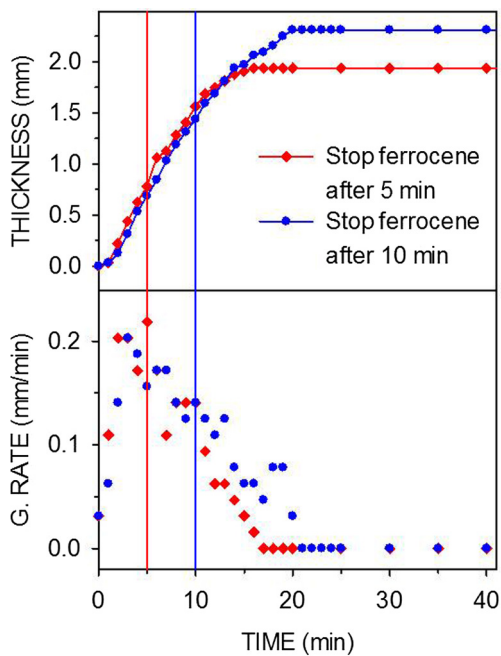


FIG. 6. The stopping of ferrocene flow at 750 °C results in growth termination independent of whether ferrocene is stopped during the growth-acceleration stage after 5 min, or past it at 10 min.

as stable reaction intermediates by chemical analysis of the feedstock composition after the thermal cracking step [43].

The autocatalytic reaction model provides a wide range of options for influencing the polymerization pathways to control the VANTA properties and postpone or eliminate growth termination through chemical means. Figure 4(b) illustrates that the most effective diagnostics for these type of experiments is real-time measurement of the rate of the decay stage. A practically useful approach for optimizing the properties of reaction end products can be envisioned by targeting directly one of the three stages and monitoring the effect on the decay rate. Although well established in standard polymerization studies, there is limited practice of this approach reported for VANTA growth. In one example, the addition of trace amounts of vinyl acetylene (C_4H_4) is shown to increase the VANTA growth rate more than any other molecule in a series of eight small hydrocarbons tested [43]. C_4H_4 is a stable molecule that is a well-known intermediate species in C_2H_2 polymerization [29,39]. The effectiveness of C_4H_4 is attributed to the fact that its molecular structure contains carbon bonding for unsaturated functionality of both alkenes and alkynes [43].

The most striking feature of C_4H_4 in acetylene polymerization is that it eliminates the induction delay, suggesting that it is effective in the initiation stage of the polymerization reaction [29]. The growth curves in Figs. 4 and 6 illustrate results of experiments that target the propagation step of the polymerization reaction. The data in Fig. 4

compare a CVD experiment in which trace amounts of ferrocene are continuously added into the C_2H_2 flow (blue line and dots) with that for water-assisted CVD growth (red line and squares) [10]. Note that the induction stage is absent in the supergrowth data because it is compiled from growth interruption steps and not by real-time measurements. After the accelerating stage is completed, supergrowth just like VANTA and any other forest growth, transitions into growth decay and growth termination. However, there is a dramatic difference in the decay rate for the two experiments. Growth termination in supergrowth is already complete after about 15–20 min while the growth in the C_2H_2 -ferrocene experiment continues for much longer, resulting in taller VANTA.

The C_2H_2 polymerization process starts with polyyne chain formation that eventually evolves into a competition between cyclization and chain propagation [44]. Promoting cyclization over random chain propagation favors the preservation of ordered structure growth in VANTA. The thermal decomposition of ferrocene provides metallocene intermediates that are known to interact catalytically with C_2H_2 to promote the formation of aromatic carbon species [45]. The transformation of five-membered rings into six-membered rings that is catalyzed by metallocenes is known to be an important step in aromatic carbon formation [46]. The data in Fig. 6 show that stopping the ferrocene flow causes termination of VANTA growth, and it makes no difference whether this is done during the growth-acceleration stage (after 5 min, red line) or during the growth decay stage (10 min, blue line), suggesting that the Fe metallocyclic intermediates, from thermal decomposition of ferrocene, interact with the propagation stage in C_2H_2 polymerization.

IV. CONCLUSIONS

The similarities in structure and properties between CNTs and polymers are widely recognized [47]. CNTs are even sometimes referred to as the ultimate polymer because of the strength and perfection afforded by the hexagonal sp^2 bonding. However, the correspondence between the two is not currently exploited by the research community for advancing the science and technology of CNTs. The perspective of CNTs as polymers enables the entire theoretical and experimental framework developed for conventional polymers to be transplanted to CNTs. In this paper we discuss an alternative approach for controlling the structure-property relationship in CNT forests from the perspective of polymerization kinetics, focused on developing a macroscopic application platform that retains the superior properties of the constituent CNTs.

The control mechanisms are derived from analysis of real-time VANTA growth kinetics, which reveals that unlike previously thought, the forest properties are dominated by the rate of carbon incorporation by acetylene

addition, instead of the dissolution and precipitation rate of carbon in metal particles. The real-time data show a regime in which VANTA growth occurs by autocatalytic kinetics suggesting radical chain polymerization as the most likely mechanism for direct addition of carbon by acetylene. Postgrowth structural analysis results, obtained from SEM imaging and SANS, support the kinetics picture indicating that the VANTA structure is determined by the extent of the polymerization process, which is characterized by the kinetic chain length that controls the CNT length. The structural analysis also reveals a cooperative effect between growth and structure that is manifested by the compressing of the polymerization product distributions during growth within a finite width imposed by the VANTA height. The most obvious example for illustration of these effects is the length distribution of CNTs. To fit within the collective VANTA height, faster growing CNTs are forced to incorporate defects into their walls, facilitating bending and undulations that ultimately result in entanglement of the CNT bundles, leading to deterioration of the alignment and order of the assembly. The consequence of this undesirable randomization of structure is the degradation of the highly anisotropic thermal and electrical conductivity and deterioration of the mechanical strength of the macroscopic assembly.

The immediate benefit from the insight provided here into the mechanism of VANTA growth is in suggesting alternative approaches for growing taller VANTA by preventing growth termination. Directly related to growing long CNTs is the need to manage the finite width of the distribution of CNT lengths, to prevent the deterioration of the constituent CNT properties. One approach that shows success in preliminary studies in our laboratory is the patterning of the growth areas. Circular patterns of diameters in range of few microns to few hundred microns are used to grow high-aspect-ratio CNT rods that serve as macroscopic wires for studying the anisotropy in thermal and electrical conductivity. The significance of this work is that by focusing on cooperative effects in growth it identifies the critical features that must be optimized in the growth process to preserve the superior properties of individual CNTs in macroscopic assemblies for high-density energy storage, heat dissipation, and advanced interconnects.

ACKNOWLEDGMENTS

This research was sponsored by the U.S. Department of Energy (DOE), Office of Science, Basic Energy Sciences, Materials Sciences and Engineering Division.

[1] W. Z. Li, S. S. Xie, L. X. Qian, B. H. Chang, B. S. Zou, W. Y. Zhou, R. A. Zhao, and G. Wang, Large-scale synthesis of aligned carbon nanotubes, *Science* **274**, 1701 (1996).

[2] G. Chen, D. N. Futaba, and K. Hata, Catalysts for the growth of carbon nanotube “forests” and superaligned arrays, *MRS Bulletin* **42**, 802 (2017).

[3] Gyula Eres, C. M. Rouleau, M. Yoon, A. A. Puzos, J. J. Jackson, and D. B. Geohegan, Model for self-assembly of carbon nanotubes from acetylene based on real-time studies of vertically aligned growth kinetics, *J. Phys. Chem. C* **113**, 15484 (2009).

[4] M. F. L. De Volder, S. H. Tawfick, R. H. Baughman, and A. J. Hart, Carbon nanotubes: Present and future commercial applications, *Science* **339**, 535 (2013).

[5] *Carbon Nanotubes Synthesis, Structure, Properties, and Applications*, edited by M. S. Dresselhaus, G. Dresselhaus, and Ph. Avouris (Springer-Verlag Berlin Heidelberg, 2001).

[6] L. Bentea, M. A. Watzky, and R. G. Finke, Sigmoidal nucleation and growth curves across nature fit by the Finke-Watzky model of slow continuous nucleation and autocatalytic growth: explicit formulas for the lag and growth times plus other key insights, *J. Phys. Chem. C* **121**, 5302 (2017).

[7] E. R. Meshot, D. W. Zwissler, N. Bui, T. R. Kuykendall, C. Wang, A. Hexemer, K. J. J. Wu, and F. Fornasiero, Quantifying the hierarchical order in self-aligned carbon nanotubes from atomic to micrometer scale, *ACS Nano* **11**, 5405 (2017).

[8] V. Balakrishnan, M. Bedewy, E. R. Meshot, S. W. Pattinson, E. S. Polsen, F. Laye, D. N. Zakharov, E. A. Stach, and A. J. Hart, Real-time imaging of self-organization and mechanical competition in carbon nanotube forest growth, *ACS Nano* **10**, 11496 (2016).

[9] G. Odian, *Principles of Polymerization*, 4th ed. (Wiley, Hoboken, NJ, 2004).

[10] Gyula Eres, A. A. Puzos, D. B. Geohegan, and H. Cui, In situ control of the catalyst efficiency in chemical vapor deposition of vertically aligned carbon nanotubes on pre-deposited metal catalyst films, *Appl. Phys. Lett.* **84**, 1759 (2004).

[11] E. R. Meshot, E. Verploegen, M. Bedewy, S. Tawfick, A. R. Woll, K. S. Green, M. Hromalik, L. J. Koerner, H. T. Philipp, M. W. Tate, S. M. Gruner, and A. J. Hart, High-speed in situ x-ray scattering of carbon nanotube film nucleation and self-organization, *ACS Nano* **6**, 5901 (2012).

[12] M. Bedewy, E. R. Meshot, M. J. Reinker, and A. J. Hart, Population growth dynamics of carbon nanotubes, *ACS Nano* **11**, 8974 (2011).

[13] T. P. J. Knowles, C. A. Waudby, G. L. Devlin, S. I. A. Cohen, A. Aguzzi, M. Vendruscolo, E. M. Terentjev, M. E. Welland, and C. M. Dobson, An analytical solution to the kinetics of breakable filament assembly, *Science* **326**, 1533 (2009).

[14] K. Hata, D. N. Futaba, K. Mizuno, T. Namai, M. Yumura, and S. Iijima, Water-assisted highly efficient synthesis of impurity-free single-walled carbon nanotubes, *Science* **306**, 1362 (2004).

[15] P. McAllister and E. E. Wolf, An activation-deactivation model for catalytic deposition of carbon, *J. Catal.* **138**, 129 (1992).

[16] A. A. Puzos, D. B. Geohegan, S. Jesse, I. N. Ivanov, and G. Eres, In situ measurements and modeling of carbon

- nanotube array growth kinetics during chemical vapor deposition, *Appl Phys. A: Mater. Sci. Process.* **81**, 223 (2005).
- [17] R. T. K. Baker, Catalytic growth of carbon filaments, *Carbon* **27**, 315 (1989).
- [18] M. H. Ruummeli, A. Bachmatiuk, F. Börrnert, F. Schäffel, I. Ibrahim, K. Cendrowski, G. Simha-Martynkova, D. Plachá, E. Borowiak-Palen, G. Cuniberti, B. Büchner, Synthesis of carbon nanotubes with and without catalyst particles, *Nanoscale Res. Lett.* **6**, 303 (2011).
- [19] J. R. Sanchez-Valencia, T. Dienel, O. Gröning, I. Shorubalko, A. Mueller, M. Jansen, K. Amsharov, P. Ruffieux, and R. Fasel, Controlled synthesis of single-chirality carbon nanotubes, *Nature* **512**, 61 (2014).
- [20] M. R. Maschmann, Integrated simulation of active carbon nanotube forest growth and mechanical compression, *Carbon* **86**, 26 (2015).
- [21] G. E. P. Box, Science and statistics, *J. Am. Stat. Assoc.* **71**, 356 (1976).
- [22] Michel Boudart, *Kinetics of Chemical Processes* (Prentice-Hall, Englewood Cliffs, NJ, 1968).
- [23] Gyula Eres, A. A. Kinkhabwala, H. Cui, D. B. Geohegan, A. A. Puzos, and D. H. Lowndes, Molecular beam-controlled nucleation and growth of vertically aligned single-wall carbon nanotube arrays, *J. Phys. Chem. B* **109**, 16684 (2005).
- [24] G. Zhong, S. Hofmann, F. Yan, H. Telg, J. H. Warner, D. Eder, C. Thomsen, W. I. Milne, and J. Robertson, Acetylene: A key growth precursor for single-walled carbon nanotube forests, *J. Phys. Chem. C* **113**, 17321 (2009).
- [25] P. W. Atkins, *Physical Chemistry*, 3rd ed. (W.H. Freeman, New York, 1986).
- [26] G. Chen, R. C. Davis, H. Kimura, S. Sakurai, M. Yumura, D. N. Futaba, and K. Hata, The relationship between the growth rate and the lifetime in carbon nanotube synthesis, *Nanoscale* **7**, 8873 (2015).
- [27] P. A. Tesner, E. Y. Robinovich, I. S. Rafalkes, and E. F. Aréfiava, Formation of carbon fibers from acetylene, *Carbon* **8**, 435 (1970).
- [28] M. Frenklach and D. Clary, Aspects of autocatalytic reaction kinetics, *Ind. Eng. Chem. Fundam.* **22**, 433 (1983).
- [29] S. W. Benson, Radical processes in the pyrolysis of acetylene, *Int. J. Chem. Kin.* **24**, 217 (1992).
- [30] F. E. Karasz, J. C. W. Chien, R. Galkiewicz, G. E. Wnek, A. J. Heeger, and A. G. MacDiarmid, Nascent morphology of polyacetylene, *Nature* **282**, 286 (1979).
- [31] M. Frenklach, Reaction mechanism of soot formation in flames, *Phys. Chem. Chem. Phys.* **4**, 2028 (2002).
- [32] D. S. N. Parker, R. I. Kaiser, T. P. Troy, and M. Ahmed, Hydrogen abstraction/acetylene addition revealed, *Angew. Chem. Int. Ed.* **53**, 7740 (2014).
- [33] Y. Wang, X. Gao, H.-J. Qian, Y. Ohta, X. Wu, G. Eres, K. Morokuma, and S. Irlé, Quantum chemical simulations reveal acetylene-based growth mechanism in the chemical vapor deposition synthesis of carbon nanotubes, *Carbon* **72**, 22 (2014).
- [34] D. A. Gomez-Gualdrón and P. B. Balbuena, The role of cap chirality in the mechanism of growth of single-wall carbon nanotubes, *Nanotechnology* **19**, 485604 (2008).
- [35] M. Picher, H. Navas, R. Arenal, E. Quesnel, E. Anglaret, and V. Jourdain, Influence of the growth conditions on the defect density of single-walled carbon nanotubes, *Carbon* **50**, 2407 (2012).
- [36] H. Wang, Z. Xu, and G. Eres, Order in vertically aligned carbon nanotube arrays, *Appl. Phys. Lett.* **88**, 213111 (2006).
- [37] A. Nepal, G. P. Singh, B. N. Flanders, and C. M. Sorensen, One-step synthesis of graphene via catalyst-free gas-phase hydrocarbon detonation, *Nanotechnology* **24**, 245602 (2013).
- [38] M. Lin, J. P. Y. Tan, C. Boothroyd, K. P. Loh, E. S. Tok, and Y.-L. Foo, Direct observation of single-walled carbon nanotube growth at the atomistic scale, *Nano Lett.* **6**, 449 (2006).
- [39] X. Xu and P. D. Pacey, An induction period in the pyrolysis of acetylene, *Phys. Chem. Chem. Phys.* **3**, 2836 (2001).
- [40] J. H. Kiefer, Comment: Radical processes in the pyrolysis of acetylene, *Int. J. Chem. Kin.* **25**, 215 (1993).
- [41] D. N. Futaba, K. Hata, T. Yamada, K. Mizuno, M. Yumura, and S. Iijima, Kinetics of water-assisted single-walled carbon nanotube synthesis revealed by a time-evolution analysis, *Phys. Rev. Lett.* **95**, 056104 (2005).
- [42] C. M. Rouleau, G. Eres, H. Cui, H. M. Christen, A. A. Puzos, and D. B. Geohegan, Altering the catalytic activity of thin metal catalyst films for controlled growth of chemical vapor deposited vertically aligned carbon nanotube arrays, *Appl. Phys. A* **93**, 1005 (2008).
- [43] D. L. Plata, E. R. Meshot, C. M. Reddy, A. J. Hart, and P. M. Gschwend, Multiple alkynes react with ethylene to enhance carbon nanotube synthesis, suggesting a polymerization-like formation mechanism, *ACS Nano* **4**, 7185 (2010).
- [44] A. J. Page, S. Irlé, and K. Morokuma, Polyene chain growth and ring collapse drives Ni-catalyzed SWNT growth: A QM/MD investigation, *J. Phys. Chem. C* **114**, 8206 (2010).
- [45] M. R. Buchmaier, Regioselective polymerization of 1-alkynes and stereoselective cyclopolymerization of α,ω -heptadiynes, *Adv. Polym. Sci.* **176**, 89 (2005).
- [46] U. H. F. Bunz, New carbon-rich organometallic architectures based on cyclobutadienecyclopentadienylcobalt and ferrocene modules, *J. Organometallic Chem.* **683**, 269 (2003).
- [47] M. J. Green, N. Behabtu, M. Pasquali, and W. W. Adams, Nanotubes as polymers, *Polymer* **50**, 4979 (2009).